

<https://doi.org/10.1038/s41698-025-00891-z>

Tertiary lymphoid structures associated with improved survival and enhanced antitumor immunity in acral melanoma

Check for updates

Xinyu Su^{1,5}, Donglin Kang^{2,5}, Jiayu Wang^{3,5}, Lin Li⁴, Rong Huang¹ & Zhengyun Zou^{1,2,3} ✉

Understanding the impact of tertiary lymphoid structures (TLSs) on acral melanoma (AM) and the tumor microenvironment (TME) is critical. We analyzed TLS features in primary AM lesions from 46 patients and identified intratumoral TLSs (intra-TLSs) in 25 patients. Intra-TLS presence was significantly associated with improved overall survival. Hematoxylin and eosin staining and multiplex immunofluorescence revealed increased T-cell and CD8⁺ T-cell infiltration and fewer tumor-associated macrophages in the TME of intra-TLS patients. Transcriptomic analysis identified a TLS-associated Th1/B-cell gene set as a predictor of survival and immunotherapy response. These findings highlight the prognostic value of intra-TLSs in AMs and suggest that targeting TLS formation could enhance immunotherapy efficacy.

Tertiary lymphoid structures (TLSs) are immune cell clusters that resemble secondary lymphoid organs (SLOs). TLSs form postnatally in non-lymphoid tissues, often at sites of chronic antigen exposure, including cancer, organ transplants, and autoimmune conditions^{1,2}. TLSs are characterized by distinct T and B cell zones, along with lymph node-like vasculature that expresses peripheral node addressin (PNAd), including mucosal addressin cell adhesion molecule 1 (MAdCAM1), vascular cell adhesion molecule 1 (VCAM1), and intercellular adhesion molecule 1 (ICAM1)^{3,4}. They support local antigen presentation and the production of effector and memory T cells, promoting both humoral and cellular antitumor immune responses⁵. Growing evidence links TLS presence to improved prognosis and enhanced response to immune checkpoint inhibitors (ICIs) in various cancer types^{4,6,7}. Additionally, the heterogeneity of TLSs, including their density, localization, and maturity, significantly impact their structural composition and immune function, shaping their role in the cancer immune landscape⁸.

Despite some studies on TLSs in melanoma, most of them have focused on TLSs in metastatic lymph nodes (LNs) or other organs, with limited analysis of primary lesions^{9–11}. Additionally, many previous studies relied on tissue microarrays, which fail to display tissue structures as clearly as digital pathology slide scanning^{9,11}. As a result, the role of TLSs, especially in primary melanoma lesions, in prognosis and immunotherapy response remains unclear.

Acral melanoma (AM) is a unique subtype of melanoma derived from melanocytes in sun-shielded areas, such as the palms, soles, and nails, and is the predominant subtype in Asians¹². Compared with cutaneous melanoma (CM), AM has a lower tumor mutation burden (TMB) and rarely possess BRAF mutations. It is also associated with a markedly immunosuppressive environment, characterized by CD8⁺ T cell depletion, increased regulatory T (Treg) cells, and CD8⁺ T cell exhaustion¹³. Consequently, AM shows a poorer response to anti-PD1 monotherapy compared to CM^{14,15}. Although TLSs have been extensively studied in melanoma, research on TLSs in AMs remains limited.

To address these gaps, we assembled a cohort of 46 AM patients and investigated TLS heterogeneity in primary lesions using hematoxylin and eosin (HE) staining and multiplex immunofluorescence (mIF). We analyzed the relationships among TLS characteristics, overall survival (OS), and immune cell infiltration within the tumor microenvironment (TME). Our findings suggest that the presence of intra-TLSs in primary lesions is associated with improved OS and enhanced immune infiltration in AMs.

Results

Baseline characteristics

A total of 46 patients with AM were included in the analysis (Table 1). The median age was 68 years (range: 43–86). The cohort included 22 males (47.8%) and 24 females (52.2%). According to the TNM staging system, 5

¹Department of the Comprehensive Cancer Center, Nanjing Drum Tower Hospital, Affiliated Hospital of Medical School, Nanjing University, Nanjing, China.

²Cancer Center, Nanjing Drum Tower Hospital Clinical College of Nanjing Medical University, Nanjing, China. ³Department of Oncology, Nanjing Drum Tower Hospital Clinical College of Nanjing University of Chinese Medicine, Nanjing, China. ⁴Department of Pathology, Nanjing Drum Tower Hospital, Affiliated Hospital of Medical School, Nanjing University, Nanjing, China. ⁵These authors contributed equally: Xinyu Su, Donglin Kang, Jiayu Wang.

✉ e-mail: zouzhenyuan@njgly.com

Table 1 | Clinicopathological factors of included patients

Factors	N = 46
Age, year	
Median (range)	68 (43–86)
Sex, No (%)	
Male	22 (47.8)
Female	24 (52.2)
TNM Stage, No (%)	
I	5 (10.8)
II	22 (47.8)
III	19 (41.4)
Follow-up time, month	
Median (range)	31.4 (7.7–124)
TLSSs, No (%)	
With	41 (89.1)
Without	5 (10.9)
Intratumoral TLSSs, No (%)	
With	25 (54.3)
Without	21 (45.7)
Peritumoral TLSSs, No (%)	
With	39 (84.8)
Without	7 (15.2)

patients (10.8%) were stage I, 22 (47.8%) were stage II, and 19 (41.4%) were stage III. The median follow-up was 31.4 months (range: 7.7–124 months).

The number, localization, and maturation of TLSSs within the TME were assessed by a pathologist using HE staining and mIF (Fig. 1A–D). TLSSs were identified in 41 patients, both peritumoral and intratumoral. The number of each feature of the TLSS is shown in Supplementary Table 1. No significant differences in intra-TLSS or peri-TLSS proportions were noted between different stages or sexes, however intra-TLSS proportions were greater in stages I–II (Supplementary Fig. 1A, B). Quantification revealed that patients in stages I–II had significantly more intra-TLSSs and eTLSSs than did those in stage III ($P = 0.053$, $P = 0.036$, respectively) (Table 2). No significant differences in the number of different features of TLSSs were observed between sexes.

Features of TLSSs correlate with OS

To examine the relationship between TLSS features and OS in AM, we categorized patients on the basis of TLSS number, localization, and maturation. Kaplan-Meier analysis revealed that patients with TLSSs had significantly longer OS than did those without TLSSs ($P = 0.032$) (Fig. 2A). However, grouping patients on the basis of the median number of TLSSs in the TME (high vs. low) revealed no significant difference in OS ($P = 0.29$) (Fig. 2B). Compared to patients without intra-TLSSs, patients with intra-TLSSs had significantly longer OS ($P = 0.037$) (Fig. 2C), whereas no significant difference in OS was noted between groups with and without peri-TLSSs ($P = 0.28$) (Fig. 2D). Finally, TLSS maturation did not correlate with OS, as no significant differences were observed among eTLSS, pTLSS, and sTLSS ($P = 0.26$, $P = 0.91$, and $P = 0.14$, respectively) (Supplementary Fig. 2A–C).

TLSS features correlate with intratumoral immune infiltrates

Research has shown that TLSSs are associated not only with OS but also with the response to ICB therapy. The response to ICB therapy is closely linked to the TME, which includes immune cells, tumor cells, and fibroblasts, all of which interact continuously¹⁶. Therefore, we analyzed the relationships between TLSS features and immune cell proportions and distributions in the TME of AMs (Fig. 3A, Supplementary Table 2). Intra-TLSSs presence was

associated with increased T cell ($CD4^+$ and $CD8^+$) and $CD8^+$ T cell infiltration in the TME (Fig. 3B, C). Conversely, peri-TLSSs was correlated with a higher proportion of $CD68^+$ macrophages (Supplementary Fig. 3B).

On the basis of the assumption that two cells are more likely to interact if the distance between their nuclei is less than $20\ \mu\text{m}$ ¹⁷ and the findings of Alberto et al.¹⁸ linking the proximity of $CD8^+$ T cells to cancer cells (within $50\ \mu\text{m}$) with the response to ICB therapy in urothelial cancer, we quantified immune cell numbers within $20\ \mu\text{m}$ and $50\ \mu\text{m}$ of tumor cells. We found that, compared with patients without intra-TLSSs, those with intra-TLSSs had significantly more $CD8^+$ T cells within a $50\ \mu\text{m}$ radius and fewer $CD68^+$ macrophages within a $20\ \mu\text{m}$ radius around tumor cells (Fig. 3D, E). Patients with sTLSSs had more $CD8^+$ T cells within $50\ \mu\text{m}$ of tumor cells (Supplementary Fig. 3C) and within $20\ \mu\text{m}$ of $CD68^+$ macrophages (Supplementary Fig. 3D).

$CD8^+$ T cells and $CD68^+$ macrophages play key roles in the TME, and their interactions influence tumor immunity. Therefore, we analyzed the relationships between TLSS features and the interactions between $CD8^+$ T cells and $CD68^+$ macrophages. Our study revealed that, compared with patients without intra-TLSSs, those with intra-TLSSs had more $CD68^+$ macrophages within $20\ \mu\text{m}$ and $50\ \mu\text{m}$ of $CD8^+$ T cells (Fig. 3F, G) and a shorter spatial distance between these two cell types (Fig. 3H). Additionally, TLSS presence was associated with a greater proportion of $CD4^+$ T cells (Supplementary Fig. 3A).

Role of the TLSS signature gene score in AM

We analyzed transcriptomic sequencing data and clinical information from Liang WS et al.’s study on AM¹⁹ to assess the impact of nine TLSS-associated signature gene sets on OS and disease-free survival (DFS) (Fig. 4A, B). The results revealed that both the Th1/B cell signature gene set and the TLSS Germinal Center Mature gene set were significantly associated with OS and DFS (Th1/B cell signature: OS: $P = 0.029$; DFS: $P = 0.039$; TLSS Germinal Center Mature: OS: $P = 0.012$; DFS: $P = 0.041$). In contrast, the TLSS gene set was significantly associated with OS ($P = 0.027$) but not with DFS ($P = 0.12$). The other gene had no significant impact on OS or DFS. When we evaluated the effects of these gene sets on OS using data from Farshidfar et al.²⁰, none were found to be associated with OS (Supplementary Fig. 4).

Given the influence of TLSSs on immunotherapy, we further explored the relationship between nine gene sets—particularly the Th1/B cell signature and TLSS Germinal Center Mature gene sets—and immunotherapy efficacy in AMs. Our analysis revealed that the Th1/B cell signature gene set was more strongly correlated with immunotherapy efficacy than the TLSS Germinal Center Mature gene set (Fig. 4C).

Discussion

In this study, we observed TLSSs in the TME of 41 out of 46 (89.13%) treatment-naïve patients with stage I–III AM. This prevalence is significantly higher than that reported in previous melanoma studies. For example, Cipponi A et al.²¹ reported TLSSs in 14 out of 29 (48%) melanoma patients. However, their study included various melanoma subtypes and focused primarily on lymph node metastases. Similarly, Lynch et al.¹¹ identified TLSSs in 30 out of 64 (47%) melanoma patients used tissue microarrays to analyze metastatic samples. In contrast, our study focused on primary tumor samples from patients with stage I–III AM, employing mIF on whole pathological sections. Vanhersecke et al. reported that mIF, along with HE and double $CD20/CD23$ staining, was the most sensitive method for detecting TLSSs²². They also reported a 2.0-fold greater likelihood of detecting TLSSs in primary tumor samples compared to metastases. Among the 41 patients with TLSSs in our study, 10 (24.4%) had sTLSSs, which is consistent with the findings of Lynch et al.¹¹. Further analysis of the relationships between clinical characteristics and TLSS numbers revealed that patients in stages I–II had greater numbers of intra-TLSSs and eTLSSs in the TME. A similar phenomenon was observed in non-small cell lung cancer, in which the number of TLSSs significantly decreased in stage III patients as compared to stage II²³. While various molecular components, such as cytokines, chemokines, and adhesion molecules, are known to play key roles in TLSS

Fig. 1 | Representative structure of TLS in AM.

A Representative H&E staining image of TLS (Indicated by the red arrow, Scale bars: 20 \times).
B Representative mIF staining image of TLS (Markers: CD20, CD21, CD23. Scale bars: 100 μ m).
C Representative mIF staining image of TLS (Markers: CD4, CD8, CD68, CD10; Scale bars: 100 μ m). **D** Representative mIF staining image of eTLS, pTLS, sTLS (left, middle, right column, respectively; Markers: CD20, CD21, CD23; Scale bars: 100 μ m). TLS tertiary lymphoid structures, AM acral melanoma, mIF multiplex immunofluorescence, eTLS early tertiary lymphoid structure, pTLS primary follicle-like TLS, sTLS secondary follicle-like TLS.

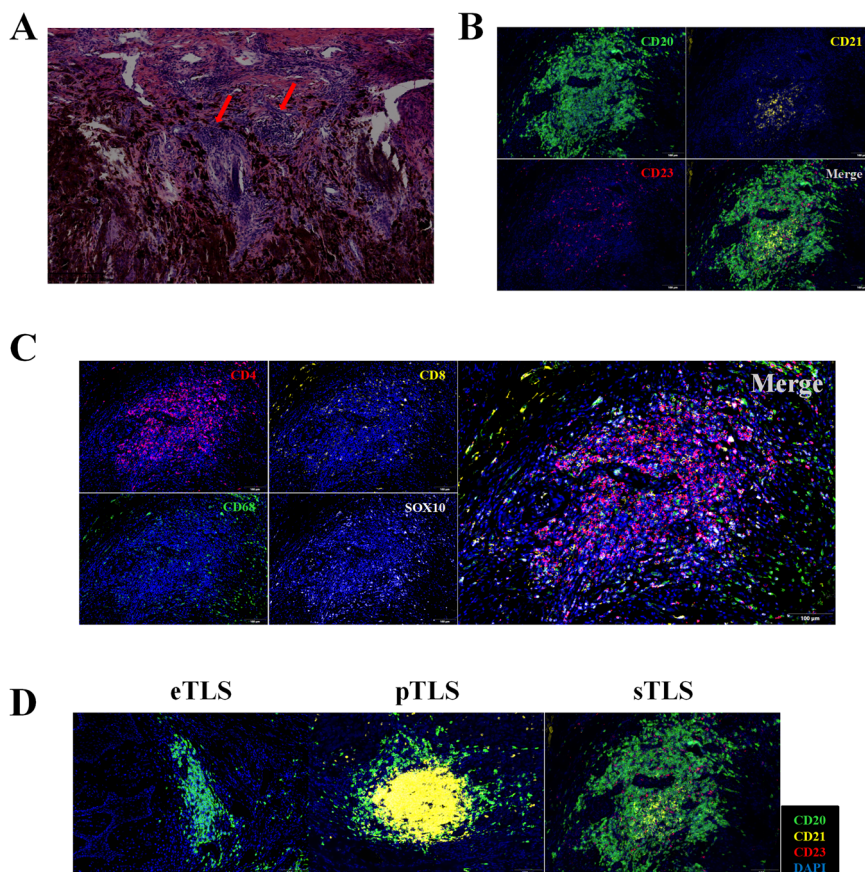


Table 2 | Association of clinical features and number of tertiary lymphoid structures in TME

Features	TNM Stage (n, mean)		P value	Sex (n, mean)		P-value
	I-II	III		Male	Female	
Total TLSs	8.930	6.530	0.123	8.820	7.130	0.378
intratumoral TLSs	4.110	2.110	0.053	4.270	2.370	0.555
intratumoral eTLSs	2.260	0.740	0.036	1.770	1.500	0.770
intratumoral pTLSs	0.700	0.470	0.094	0.950	0.290	0.453
intratumoral sTLSs	1.150	0.890	0.528	1.550	0.580	0.570
peritumoral TLSs	4.810	4.420	0.840	4.550	4.750	0.956
peritumoral eTLSs	3.150	2.470	0.838	2.590	3.130	0.577
peritumoral pTLSs	0.780	0.790	0.762	0.730	0.830	0.641
peritumoral sTLSs	0.890	1.160	0.841	1.230	0.790	0.527

formation, the underlying mechanisms remain unclear²⁴. Notably, although each chemokine independently induces TLS, it produces structures with distinct characteristics. For example, CXCL13 induces B cell aggregates that lack FDC networks, whereas TNF and CXCL12 induce small lymphocytic infiltrates, predominantly B cells with few T cells, and, in the case of CXCL12, DCs^{25,26}. Furthermore, the CCR7 ligands CCL19 and CCL21 induce similar aggregates, but CCL21 produces larger, more organized structures²⁶.

Advances in mIF now allow for detailed evaluation of TLSs in the TME, including their size, density, localization, composition, and maturity. TLS presence has been linked to a better prognosis in cancers such as lung adenocarcinoma²⁷, melanoma¹¹, and dedifferentiated liposarcoma²⁸. High-density TLSs are associated with a better prognosis in non-metastatic

colorectal cancer²⁹. In cancers such as intrahepatic cholangiocarcinoma, breast cancer, and hepatocellular carcinoma, intra-TLS is correlated with a better prognosis, whereas peri-TLS is linked to poorer outcomes³⁰⁻³³. In our study, only intra-TLSs in AM patients were associated with improved OS, while peri-TLSs showed no correlation. Additionally, neither the number nor the maturity of TLSs affected OS. These results are limited by the small sample size, highlighting the need for larger studies to further investigate the role of TLSs in patient outcomes.

TLSs play a crucial role in the antitumor immune response by facilitating antigen presentation to T cells via dendritic cells (DCs) and promoting the activation, proliferation, and differentiation of T and B cells⁴. T cells within TLSs exhibit increased activation markers compared with other tumor-resident T cells in melanoma³⁴. In murine melanoma models, TLS-driven tumor-specific T cell responses led to immune cell infiltration and tumor regression^{35,36}. Additionally, TLS-associated fibroblasts and other cell subsets secrete survival factors that support lymphocyte homeostasis, potentially contributing to the persistence of tumor-reactive T cells^{37,38}. Our study found that patients with intra-TLSs had significantly greater proportions of T and CD8⁺ T cells in the TME compared to those without intra-TLSs. Similarly, a melanoma study revealed increased densities of CD8⁺ T cells, B cells, and plasma B cells in TLS⁺ cutaneous melanoma metastases (CMMs). They also observed that intratumoral CD8⁺ T cell density was correlated with a higher proportion of sTLSs, but not eTLSs or pTLSs¹¹.

Although genetic and epigenetic alterations are commonly considered the root causes of cancer, their progression is also closely linked to crosstalk among tumor cells, immune cells, and the extracellular matrix (ECM)³⁹. CD8⁺ T cells and tumor-associated macrophages (TAMs) are key immune cells in the TME. CD8⁺ T cells typically exert antitumor effects, while TAMs often promote tumor progression. The interactions between these cells and tumor cells influence cancer prognosis and affect the efficacy of therapeutic interventions⁴⁰. Zhu et al. found that higher densities of CD8⁺ tumor-infiltrating lymphocytes within 20 μ m of melanoma cells were associated

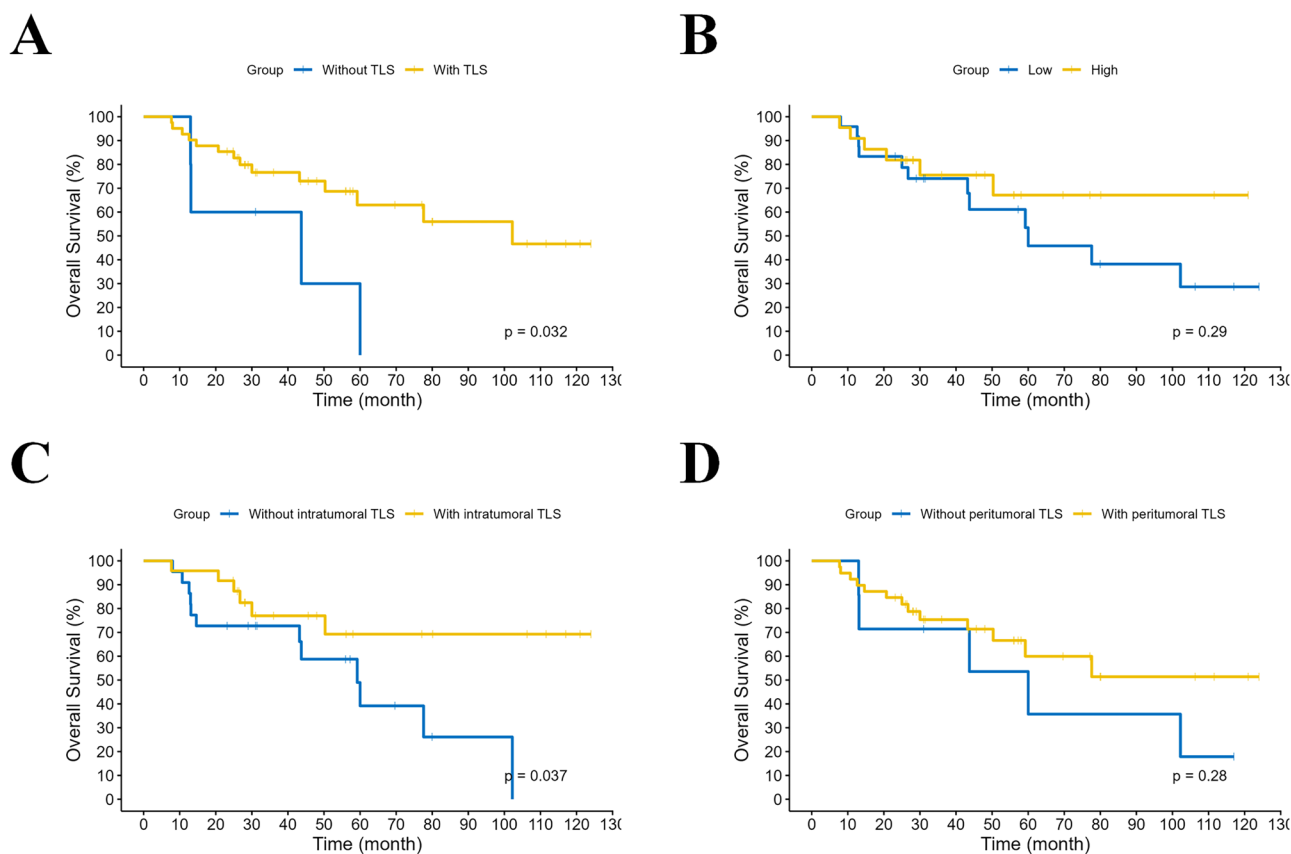


Fig. 2 | Kaplan-meier analysis of the relationship between TLS features and overall survival in AM Patients. **A** Kaplan-Meier survival analysis of the cohort grouped by the presence of TLS. **B** Kaplan-Meier survival analysis of the cohort grouped by the number of TLS. **C** Kaplan-Meier survival analysis of the cohort

grouped by the presence of intratumoral TLS. **D** Kaplan-Meier survival analysis of the cohort grouped by the presence of peritumoral TLS. TLS tertiary lymphoid structures, AM acral melanoma.

with a good response to anti-PD-1 immunotherapy and improved progression-free survival (PFS)⁴¹. Wang et al. showed that PD-L1⁻ TAMs, compared with PD-L1⁺ TAMs, interact more frequently with cancer cells and promote tumor progression¹⁷. Our study revealed that patients with sTLSs had more CD8⁺ T cells surrounding tumor cells, suggesting that TLS maturation may be linked to CD8⁺ T cell infiltration around tumors, despite the lack of an overall increase in CD8⁺ T cell proportion in the TME. Crosstalk between TAMs and CD8⁺ T cells is commonly observed in the TME. TAMs can modulate T cell responses by releasing CXCL9, CXCL10, IL-12, IL-15, and IL-18^{42,43}, or by expressing T cell immunoglobulin and mucin domain-containing molecule 4 (TIM4) to constrain CD8⁺ T cells proliferation and activation⁴⁴. FOLR2⁺ macrophages in perivascular tumor areas interact with CD8⁺ T cells and efficiently prime effector CD8⁺ T cells⁴⁵. However, Kersten et al. reported that TAMs and CD8⁺ T cells engage in long-lasting, antigen-specific synaptic interactions that do not activate T cells but rather prime them for exhaustion⁴⁶. In our study, patients with intra-TLSs had a significantly higher number of CD68⁺ macrophages surrounding CD8⁺ T cells in the TME, and a closer distance between the two cell types. However, the role of the interaction between CD68⁺ macrophages and CD8⁺ T cells in melanoma still requires further investigation.

Our study, along with previous research, demonstrated that TLSs serve as both prognostic markers and indicators of the tumor immune micro-environment (TIME), making them promising targets for cancer therapy. Understanding TLS formation and maturation is crucial, and recent advances in spatial transcriptomics and proteomics offer new insights. We compiled nine TLS signature gene sets, including the Th1/B cell and TLS Germinal Center Mature signatures, which predict patient prognosis and immunotherapy efficacy. The Th1/B cell signature shows strong potential for predicting treatment response, suggesting that Th1-B cell interactions

play a key role in TLS formation. The immune infiltrate in tumors in which TLSs are present is often skewed toward a TH1 or cytotoxic effector state⁴⁷. However, owing to the lack of spatial data in AM, studying these gene sets at the spatial level remains a challenge. As omics technologies advance, they will deepen our understanding of TLSs and accelerate progress in precision medicine.

In summary, this study is the first to comprehensively assess TLSs in AM patients and their clinicopathological associations. Our findings suggest that intra-TLS can serve as a prognostic marker and may contribute to an immune-responsive microenvironment. These insights open the door for therapeutic strategies aimed at enhancing TLS function, potentially improving clinical outcomes and increased responses to immunotherapy. However, due to the limited sample size, further studies with a larger cohort are needed to confirm and provide deeper insights into how TLSs influence immune cell infiltration in AMs.

Methods

Patients and clinical data collection

This study included a cohort of 46 patients diagnosed with acral melanoma (AM), all of whom were treated at the Nanjing Drum Tower Hospital, Affiliated Hospital of Medical School, Nanjing University. Patient enrollment spanned from January 2013 to June 2021, with a follow-up period extending until December 2023. All participants self-reported no prior history of cancer or any antitumor therapy before the surgical resection of their primary lesion. The clinicopathological features evaluated in this study included age, sex, and tumor stage (Table 1). The clinical stage of AM was determined in accordance with the 7th edition of the American Joint Committee on Cancer (AJCC) staging system. Overall survival (OS) was defined as the time interval from the date of surgical treatment to the date of

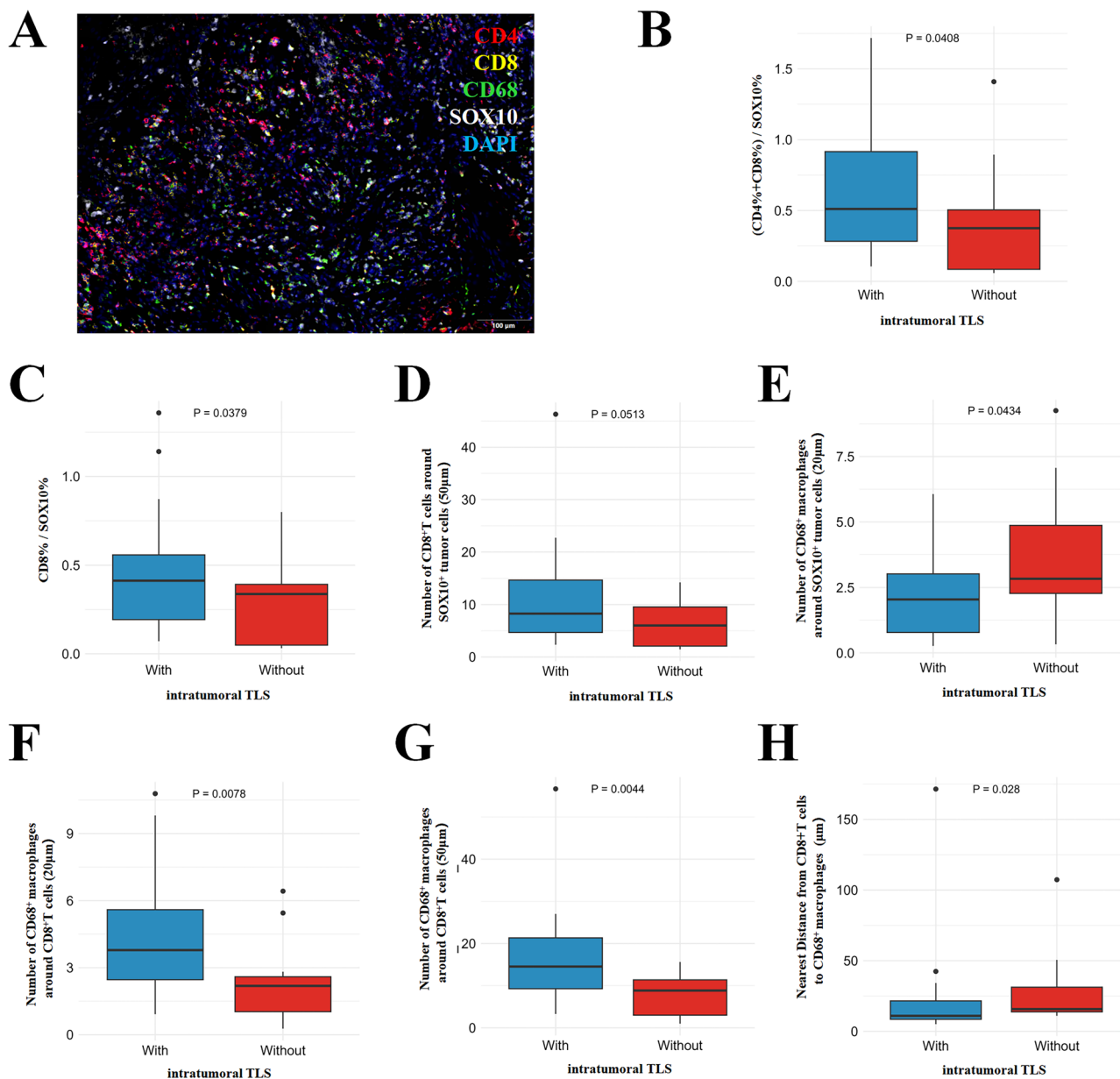


Fig. 3 | Association between intratumoral TLS and immune infiltrates in AM. **A** Representative mIF image of immune infiltrates in AM. **B** Proportion of T cells (CD4⁺ and CD8⁺). **C** Proportion of CD8⁺ T cells. **D** Number of CD8⁺ T cells within 50µm of SOX10⁺ tumor cells. **E** Number of CD68⁺ Macrophages within 20µm of

SOX10⁺ tumor cells. **F** Number of CD68⁺ Macrophages within 20µm of CD8⁺ T cells. **G** Number of CD68⁺ Macrophages within 50µm of CD8⁺ T cells. **H** Nearest distance from CD8⁺ T cells to CD68⁺ macrophages (unit: µm). TLS tertiary lymphoid structures; AM acral melanoma; mIF multiplex immunofluorescence.

patient death during the follow-up period. This study adheres to the *Guidance of the Ministry of Science and Technology (MOST) for the Review and Approval of Human Genetic Resources*. All patient materials were sampled and handled in compliance with the ethical principles of the Declaration of Helsinki. This included obtaining written informed consent from all donors and securing approval from the Institute Research Ethics Committees of the Affiliated Drum Tower Hospital of Nanjing University Medical School (Approval No. 2019-312-01).

Multiplex immunofluorescence staining and image analysis

For mIF analysis, we used a PANO 5-plex IHC kit based on tyramide signal amplification (TSA) following the manufacturer’s protocol (Panovue, China). Consecutive 4-µm thick sections from formalin-fixed paraffin-embedded (FFPE) tumor specimens were stained. Multiplexed images of each stained slide were captured using the PanoVIEW VS200 System

(Panovue, China). Acidic and alkaline antigen retrieval buffers (Panovue, China) were applied as necessary. The staining sequences and antibodies used are listed in Supplementary Table 3.

The multispectral images were spectrally unmixed using single-stain positive control images with the InForm software (Akoya Biosciences, Marlborough, Massachusetts, USA). The immune cell proportions in the tumor microenvironment (TME) were quantified as the percentage of positively stained cells among all nucleated cells. The normalized proportion of immune cells was calculated by dividing the immune cell proportion by the tumor cell proportion (e.g., the proportion of CD8⁺ T cells = CD8⁺/SOX10⁺ cells). Data for downstream analysis included the position of each cell (x- and y-coordinates of the nuclei) and its corresponding cell type. Spatial relationships between cells in the TME were examined using the first-nearest neighbor (1-NN) statistic, implemented in spatstats. mIF staining assay results were validated in at least three biological replicates.

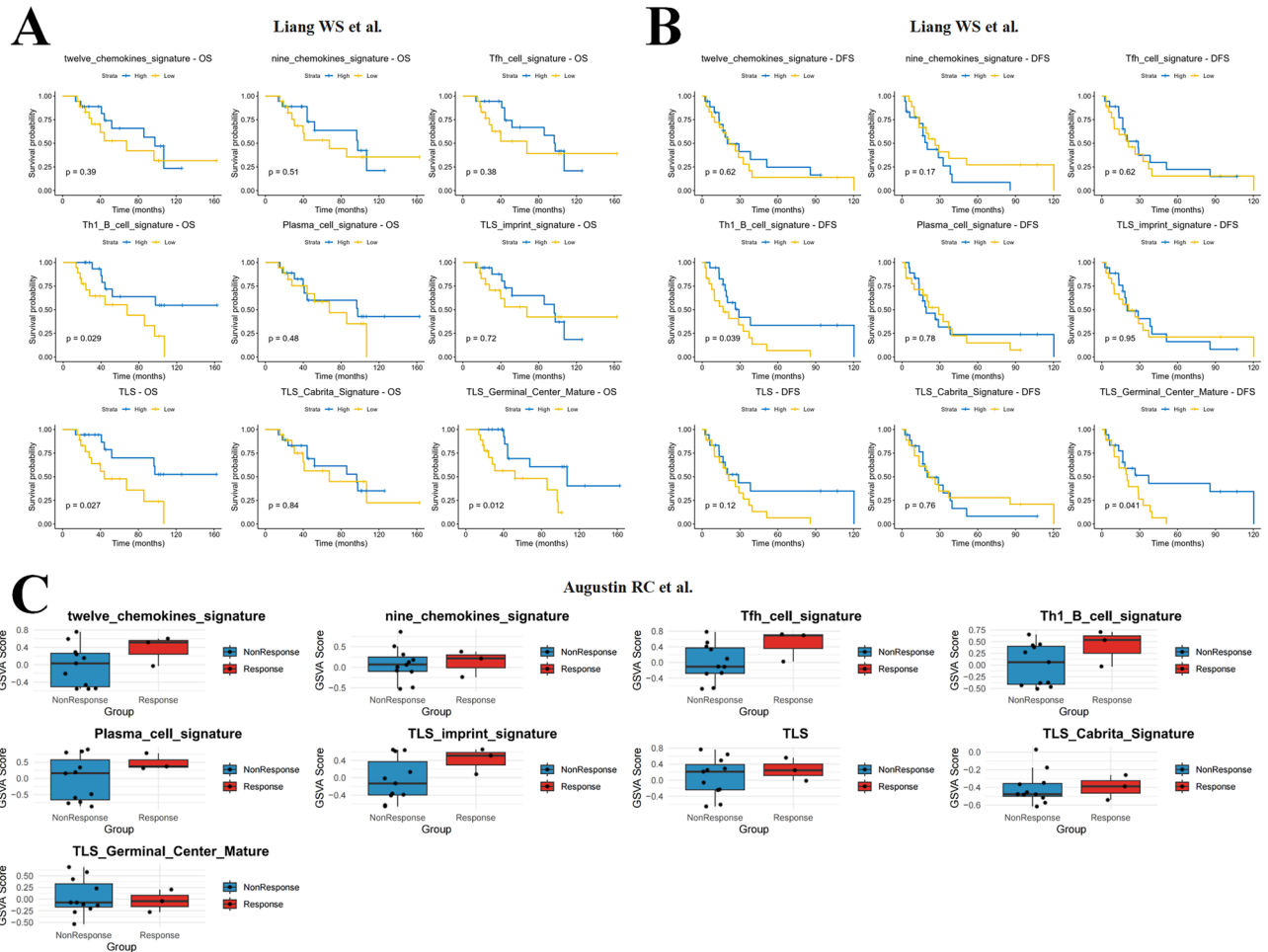


Fig. 4 | Association of nine TLS-associated signature gene sets with prognosis and immunotherapy efficacy in AM patients. A Kaplan-Meier curve analysis of the relationship between TLS-associated signature gene sets and OS. B Kaplan-Meier curve analysis of the relationship between TLS-associated signature gene sets and

DFS. C Differences in TLS-associated signature gene scores between the response and non-response groups to immunotherapy. TLS tertiary lymphoid structures, AM acral melanoma, OS overall survival, DFS disease-free survival.

Defining TLS and TLS features

First, lymphoid aggregates were observed on whole-slide images (WSIs) (Fig. 1A). TLSs feature a central CD20⁺ B cell zone encircled by CD3⁺ T cells⁷. Using mIF with CD20/CD21/CD23 markers, we first delineated the inner B cell zone (Fig. 1B). Subsequent mIF analysis of consecutive sections stained with CD4/CD8/CD68 confirmed the peripheral organization of CD4⁺ and CD8⁺ T cells around this core structure (Fig. 1C), thereby establishing TLS identification. The tumor invasive margins were identified using a combination of H&E staining and mIF (tumor cells: SOX10⁺ cells). TLS were classified into peritumoral TLSs (peri-TLSs) and intratumoral TLSs (intra-TLSs) on the basis of their location relative to the invasive margins of the tumor⁷. TLS maturation is a dynamic, multi-stage process starting from immature early TLSs (eTLSs), to primary follicle-like TLSs (pTLSs), to secondary follicle-like TLSs (sTLSs)⁴⁸. As previously described⁴¹, the maturation state of TLSs can be categorized into eTLS, pTLS, and sTLS on the basis of the presence of a CD21⁺ follicular dendritic cell (FDC) network (pTLS), a CD23⁺ germinal center (sTLS), or the absence of these features (eTLS) (Fig. 1D). Based on the varying maturation states of peritumoral TLSs, they were further categorized into peritumoral eTLSs, pTLSs, and sTLSs. Similarly, intratumoral TLSs were classified into intratumoral eTLSs, pTLSs, and sTLSs.

Defining the signature score of the TLS signature gene

Single-sample gene set enrichment analysis (ssGSEA)⁴⁹ was used to calculate the absolute enrichment score of the TLS signature genes, which were derived from relevant studies and are listed in Supplementary Table 4⁵⁰⁻⁵⁵.

Statistical analysis

All the statistical analyses were conducted using R version 4.2.3, SPSS version 25, and GraphPad Prism version 9. The Student’s t-test and the Mann–Whitney U test were utilized to calculate P values. Overall survival was analyzed using Kaplan–Meier and log-rank survival analyses. All the statistical tests were two-sided, with P < 0.05 considered statistically significant.

Data availability

The AM RNA-seq datasets mentioned above can be downloaded from NCBI GEO under the accession numbers GSE162682 and GSE243238, and from the dbGAP database under the accession code phs001036.v1.p1. The remaining data are available within the Article, Supplementary Information, or from the authors upon request.

Received: 25 September 2024; Accepted: 31 March 2025;

Published online: 09 April 2025

References

1. Paijens, S. T., Vledder, A., de Bruyn, M. & Nijman, H. W. Tumor-infiltrating lymphocytes in the immunotherapy era. *Cell. Mol. Immunol.* **18**, 842–859 (2021).
2. Pitzalis, C., Jones, G. W., Bombardieri, M. & Jones, S. A. Ectopic lymphoid-like structures in infection, cancer and autoimmunity. *Nat. Rev. Immunol.* **14**, 447–462 (2014).

3. Engelhard, V. H. et al. Immune Cell Infiltration and Tertiary Lymphoid Structures as Determinants of Antitumor Immunity. *J. Immunol. (Baltim., Md: 1950)* **200**, 432–442 (2018).
4. Sautès-Fridman, C., Petitprez, F., Calderaro, J. & Fridman, W. H. Tertiary lymphoid structures in the era of cancer immunotherapy. *Nat. Rev. Cancer* **19**, 307–325 (2019).
5. Fridman, W. H., Pagès, F., Sautès-Fridman, C. & Galon, J. The immune contexture in human tumours: impact on clinical outcome. *Nat. Rev. Cancer* **12**, 298–306 (2012).
6. Patil, N. S. et al. Intratumoral plasma cells predict outcomes to PD-L1 blockade in non-small cell lung cancer. *Cancer cell* **40**, 289–300.e4 (2022).
7. Schumacher, T. N. & Thommen, D. S. Tertiary lymphoid structures in cancer. *Sci. (N.Y., NY)* **375**, eabf9419 (2022).
8. Zhang, Y. et al. Tertiary lymphoid structural heterogeneity determines tumour immunity and prospects for clinical application. *Mol. Cancer* **23**, 75 (2024).
9. Cabrita, R. et al. Tertiary lymphoid structures improve immunotherapy and survival in melanoma. *Nature* **577**, 561–565 (2020).
10. Ladányi, A. et al. Ectopic lymphoid structures in primary cutaneous melanoma. *Pathol. Oncol. Res.: POR* **20**, 981–985 (2014).
11. Lynch et al. Heterogeneity in tertiary lymphoid structure B-cells correlates with patient survival in metastatic melanoma. *J. Immunother. Cancer* **9**, <https://doi.org/10.1136/jitc-2020-002273> (2021).
12. Chen, Y. A. et al. Translational pathology, genomics and the development of systemic therapies for acral melanoma. *Semin. cancer Biol.* **61**, 149–157 (2020).
13. Zhang, C. et al. A single-cell analysis reveals tumor heterogeneity and immune environment of acral melanoma. *Nat. Commun.* **13**, 7250 (2022).
14. Nakamura, Y. et al. Anti-PD1 checkpoint inhibitor therapy in acral melanoma: a multicenter study of 193 Japanese patients. *Ann. Oncol. : Off. J. Eur. Soc. Med. Oncol.* **31**, 1198–1206 (2020).
15. Hamid, O. et al. Safety and tumor responses with lambrolizumab (anti-PD-1) in melanoma. *N. Engl. J. Med.* **369**, 134–144 (2013).
16. Hiam-Galvez, K. J., Allen, B. M. & Spitzer, M. H. Systemic immunity in cancer. *Nat. Rev. Cancer* **21**, 345–359 (2021).
17. Wang, L. et al. PD-L1-expressing tumor-associated macrophages are immunostimulatory and associate with good clinical outcome in human breast cancer. *Cell Rep. Med.* **5**, 101420 (2024).
18. Gil-Jimenez, A. et al. Spatial relationships in the urothelial and head and neck tumor microenvironment predict response to combination immune checkpoint inhibitors. *Nat. Commun.* **15**, 2538 (2024).
19. Liang, W. S. et al. Integrated genomic analyses reveal frequent TERT aberrations in acral melanoma. *Genome Res.* **27**, 524–532 (2017).
20. Farshidfar, F. et al. Integrative molecular and clinical profiling of acral melanoma links focal amplification of 22q11.21 to metastasis. *Nat. Commun.* **13**, 898 (2022).
21. Cipponi, A. et al. Neogenesis of lymphoid structures and antibody responses occur in human melanoma metastases. *Cancer Res.* **72**, 3997–4007 (2012).
22. Vanhersecke, L. et al. Standardized Pathology Screening of Mature Tertiary Lymphoid Structures in Cancers. *Lab. Investig.; a J. Tech. methods Pathol.* **103**, 100063 (2023).
23. Rakaee, M. et al. Tertiary lymphoid structure score: a promising approach to refine the TNM staging in resected non-small cell lung cancer. *Br. J. cancer* **124**, 1680–1689 (2021).
24. Khanal, S., Wieland, A. & Gunderson, A. J. Mechanisms of tertiary lymphoid structure formation: cooperation between inflammation and antigenicity. *Front. Immunol.* **14**, 1267654 (2023).
25. Luther, S. A., Lopez, T., Bai, W., Hanahan, D. & Cyster, J. G. BLC expression in pancreatic islets causes B cell recruitment and lymphotoxin-dependent lymphoid neogenesis. *Immunity* **12**, 471–481 (2000).
26. Luther, S. A. et al. Differing activities of homeostatic chemokines CCL19, CCL21, and CXCL12 in lymphocyte and dendritic cell recruitment and lymphoid neogenesis. *J. Immunol. (Baltim., Md : 1950)* **169**, 424–433 (2002).
27. Tamiya, Y. et al. The impact of tertiary lymphoid structures on clinicopathological, genetic and gene expression characteristics in lung adenocarcinoma. *Lung cancer (Amst., Neth.)* **174**, 125–132 (2022).
28. Tseng, W. W. et al. Analysis of the intratumoral adaptive immune response in well differentiated and dedifferentiated retroperitoneal liposarcoma. *Sarcoma* **2015**, 547460 (2015).
29. Wang, Q. et al. Peritumoral tertiary lymphoid structure and tumor stroma percentage predict the prognosis of patients with non-metastatic colorectal cancer. *Front. Immunol.* **13**, 962056 (2022).
30. Sofopoulos, M. et al. The prognostic significance of peritumoral tertiary lymphoid structures in breast cancer. *Cancer Immunol., Immunother. : CII* **68**, 1733–1745 (2019).
31. Zhang, T. et al. Peritumor tertiary lymphoid structures are associated with infiltrating neutrophils and inferior prognosis in hepatocellular carcinoma. *Cancer Med.* **12**, 3068–3078 (2023).
32. Ding, G. Y. et al. Distribution and density of tertiary lymphoid structures predict clinical outcome in intrahepatic cholangiocarcinoma. *J. Hepatol.* **76**, 608–618 (2022).
33. Shang, T. et al. Tertiary lymphoid structures predict the prognosis and immunotherapy response of cholangiocarcinoma. *Front. Immunol.* **14**, 1166497 (2023).
34. Helmink, B. A. et al. B cells and tertiary lymphoid structures promote immunotherapy response. *Nature* **577**, 549–555 (2020).
35. Schrama, D. et al. Targeting of lymphotoxin-alpha to the tumor elicits an efficient immune response associated with induction of peripheral lymphoid-like tissue. *Immunity* **14**, 111–121 (2001).
36. Schrama, D. et al. Immunological tumor destruction in a murine melanoma model by targeted LTA independent of secondary lymphoid tissue. *Cancer Immunol., Immunother. : CII* **57**, 85–95 (2008).
37. Barone, F. et al. Stromal Fibroblasts in Tertiary Lymphoid Structures: A Novel Target in Chronic Inflammation. *Front. Immunol.* **7**, 477 (2016).
38. Buckley, C. D., Barone, F., Nayar, S., Bénézec, C. & Caamaño, J. Stromal cells in chronic inflammation and tertiary lymphoid organ formation. *Annu. Rev. Immunol.* **33**, 715–745 (2015).
39. Zou, S. et al. Targeting STAT3 in Cancer Immunotherapy. *Mol. cancer* **19**, 145 (2020).
40. Su, J. et al. Cell-cell communication: new insights and clinical implications. *Signal Transduct. Target. Ther.* **9**, 196 (2024).
41. Gide, T. N. et al. Close proximity of immune and tumor cells underlies response to anti-PD-1 based therapies in metastatic melanoma patients. *Oncoimmunology* **9**, 1659093 (2020).
42. Molgora, M. & Colonna, M. Turning enemies into allies—reprogramming tumor-associated macrophages for cancer therapy. *Med (N. Y., NY)* **2**, 666–681 (2021).
43. Mantovani, A., Allavena, P., Marchesi, F. & Garlanda, C. Macrophages as tools and targets in cancer therapy. *Nat. Rev. Drug Discov.* **21**, 799–820 (2022).
44. Chow, A. et al. Tim-4(+) cavity-resident macrophages impair anti-tumor CD8(+) T cell immunity. *Cancer cell* **39**, 973–88.e9 (2021).
45. Nalio Ramos, R. et al. Tissue-resident FOLR2(+) macrophages associate with CD8(+) T cell infiltration in human breast cancer. *Cell* **185**, 1189–207.e25 (2022).
46. Kersten, K. et al. Spatiotemporal co-dependency between macrophages and exhausted CD8(+) T cells in cancer. *Cancer cell* **40**, 624–38.e9 (2022).
47. Goc, J., Fridman, W. H., Sautès-Fridman, C. & Dieu-Nosjean, M. C. Characteristics of tertiary lymphoid structures in primary cancers. *Oncoimmunology* **2**, e26836 (2013).
48. Wang, S. et al. Tertiary lymphoid structures in cancer: immune mechanisms and clinical implications. *MedComm (2020)* **5**, e489 (2024).

49. Barbie, D. A. et al. Systematic RNA interference reveals that oncogenic KRAS-driven cancers require TBK1. *Nature* **462**, 108–112 (2009).
50. Coppola, D. et al. Unique ectopic lymph node-like structures present in human primary colorectal carcinoma are identified by immune gene array profiling. *Am. J. Pathol.* **179**, 37–45 (2011).
51. Kroeger, D. R., Milne, K. & Nelson, B. H. Tumor-Infiltrating Plasma Cells Are Associated with Tertiary Lymphoid Structures, Cytolytic T-Cell Responses, and Superior Prognosis in Ovarian Cancer. *Clin. Cancer Res. : Off. J. Am. Assoc. Cancer Res.* **22**, 3005–3015 (2016).
52. Meylan, M. et al. Tertiary lymphoid structures generate and propagate anti-tumor antibody-producing plasma cells in renal cell cancer. *Immunity* **55**, 527–41.e5 (2022).
53. Gu-Trantien, C. et al. CD4⁺ follicular helper T cell infiltration predicts breast cancer survival. *J. Clin. Investig.* **123**, 2873–2892 (2013).
54. Hennequin, A. et al. Tumor infiltration by Tbet⁺ effector T cells and CD20⁺ B cells is associated with survival in gastric cancer patients. *Oncoimmunology* **5**, e1054598 (2016).
55. Ma, Y. et al. Integrating Tertiary Lymphoid Structure-Associated Genes into Computational Models to Evaluate Prognostication and Immune Infiltration in Pancreatic Cancer. *J. Leukocyte Biol.* <https://doi.org/10.1093/jleuko/qiae067> (2024).

Acknowledgements

This study was supported by the Social Development Fund of Jiangsu Province (No.BE2019605), the National Natural Science Foundation of China (No.81872484, No.82073365), and the Single Disease Database Construction Project (No. 2024-LCYJ-DBZ-01) of Nanjing Drum Tower Hospital.

Author contributions

Z.Y.Z. and X.Y.S. conceived the study concept and design. X.Y.S., D.L.K., J.Y.W. and R.H. contributed to clinical information and clinical follow-up. X.Y.S. performed the experiments. X.Y.S. and D.L.K. performed statistical analysis. L.L. was responsible for pathological diagnosis. X.Y.S. drafted the article. Z.Y.Z. was responsible for manuscript review and editing. All authors have agreed to the final version of the manuscript.

Competing interests

The authors declare no competing interests.

Additional information

Supplementary information The online version contains supplementary material available at <https://doi.org/10.1038/s41698-025-00891-z>.

Correspondence and requests for materials should be addressed to Zhengyun Zou.

Reprints and permissions information is available at <http://www.nature.com/reprints>

Publisher's note Springer Nature remains neutral with regard to jurisdictional claims in published maps and institutional affiliations.

Open Access This article is licensed under a Creative Commons Attribution-NonCommercial-NoDerivatives 4.0 International License, which permits any non-commercial use, sharing, distribution and reproduction in any medium or format, as long as you give appropriate credit to the original author(s) and the source, provide a link to the Creative Commons licence, and indicate if you modified the licensed material. You do not have permission under this licence to share adapted material derived from this article or parts of it. The images or other third party material in this article are included in the article's Creative Commons licence, unless indicated otherwise in a credit line to the material. If material is not included in the article's Creative Commons licence and your intended use is not permitted by statutory regulation or exceeds the permitted use, you will need to obtain permission directly from the copyright holder. To view a copy of this licence, visit <http://creativecommons.org/licenses/by-nc-nd/4.0/>.

© The Author(s) 2025